# Equilibrium Phase Behavior of a Continuous-Space Microphase Former

Yuan Zhuang,[1] Kai Zhang,[2] and Patrick Charbonneau[1,3]
[1]Department of Chemistry, Duke University, Durham, North Carolina 27708, USA
[2]Department of Chemical Engineering, Columbia University, New York, New York 10027, USA
[3]Department of Physics, Duke University, Durham, North Carolina 27708, USA
(Received 16 November 2015; published 29 February 2016)

Periodic microphases universally emerge in systems for which short-range interparticle attraction is frustrated by long-range repulsion. The morphological richness of these phases makes them desirable material targets, but our relatively coarse understanding of even simple models hinders controlling their assembly. We report here the solution of the equilibrium phase behavior of a microscopic microphase former through specialized Monte Carlo simulations. The results for cluster crystal, cylindrical, double gyroid, and lamellar ordering qualitatively agree with a Landau-type free energy description and reveal the nontrivial interplay between cluster, gel, and microphase formation.

DOI: 10.1103/PhysRevLett.116.098301

Microphases supersede simple gas-liquid coexistence when short-range interparticle attraction is frustrated by long-range repulsion (SALR). The resulting structures are both elegant and remarkably useful [1]. Block copolymers [2–4], for instance, form a rich array of periodic structures, such as lamellae, gyroid [5,6], and exotic morphologies [7–11], whose robust assembly enables industrial applications in drug delivery [12,13] and nanoscale patterning [14,15], among others. Because microphase formation constitutes a universality class of sorts [16], many other systems either exhibit or share the potential to form similar assemblies [1,17]. In the latter category, colloidal suspensions are particularly interesting. The relative ease with which interactions between colloids can be tuned indeed suggests that a broad array of ordered microphases should be achievable [17]. Yet, in experiments [18–20] only amorphous gels and clusters have been observed in systems ranging from proteins [21] to micron-scale beads [22].

A variety of explanations have been advanced to explain the difficulty of assembling periodic microphases in colloids, including a glasslike dynamical slowdown upon approaching the microphase regime [23,24], the existence of an equilibrium gel phase [25,26], and the dynamical arrest of partly assembled structures due either to particle-scale sluggishness [27–29] or competition between morphologies [30–32]. In order to obtain a clearer physical picture of these effects and thus hopefully guide experimental microphase ordering, a better understanding of the relationship between equilibrium statics and dynamics is needed. Insights from theory and simulation would be beneficial, but both approaches face serious challenges. On the one hand, theoretical descriptions, such as the density-functional theory [2,5,6], self-consistent field theory [33], random-phase approximation [34,35], and others [26,36], capture reasonably well the microphase structures, but corresponding dynamical descriptions are more limited [24,28,37–39]. On the other hand, the dynamics of particle-based models has been extensively studied by simulations [25,27,40–42], but our thermodynamic grasp of these models is rather poor [43–45]. In this Letter, we introduce the components needed to study the thermodynamic behavior of microscopic, microphase-forming models and thus help clarify the interplay between equilibrium ordering and sluggish dynamics.

*Simulations.*—The square-well-linear (SWL) model we study here has a schematic interaction form that can be smoothly transformed into that of diblock copolymers and other microphase-forming models. Its radial pair interaction $u(r) = u_{\mathrm{HS}}(r) + u_{\mathrm{SALR}}(r)$ includes hard-sphere volume exclusion $u_{\mathrm{HS}}(r)$ at the particle diameter $\sigma$, which sets the unit of length, as well as a SALR contribution

$$u_{\mathrm{SALR}}(r) = \begin{cases} -\varepsilon, & r < \lambda\sigma, \\ \xi\varepsilon(\kappa - r/\sigma), & \lambda\sigma < r < \kappa\sigma, \\ 0, & r > \kappa\sigma. \end{cases} \quad (1)$$

The square-well attraction strength $\varepsilon$, which sets the unit of energy, is felt up to $\lambda\sigma$; beyond that point, repulsion of strength $\xi\varepsilon$ takes over and decays linearly. Note that choosing $\xi = 0.05$ places the system well above the Lifshitz point, $\xi_L = 0.025(5)$, for the prototypical values $\lambda = 1.5$ and $\kappa = 4$ used here [1,46,49,50]. We simulate systems containing between $N = 800$ and 8000 particles under periodic boundary conditions at fixed temperature $T = 1/\beta$ (the Boltzmann constant is set to unity), fixing either pressure $p$ or volume $V$ (and thus number density $\rho = N/V$). For each state point, we perform between $10^5$ and $10^6$ Monte Carlo (MC) sweeps, which include nonstandard MC moves [51–54], in order to obtain equilibrium configurations of the different phases studied [46]. The results presented here have been first equilibrated and then

 

averaged over simulations at least 5 times longer than the structural relaxation time.

Obtaining equilibrium information about microscopic SALR particle-based models requires going beyond the common free energy techniques used for simulating gas, liquids, and crystals [53], because these techniques fail to account for the fluctuating occupancy of periodic microphase features [55]. The problem is similar to that encountered in multiple-occupancy crystals [44] and lattices with vacancies [56]. We thus consider an expanded differential form for the Helmholtz free energy per particle [44]:

$$df_c = -sdT - pd(1/\rho) + \mu_c dn_c, \tag{2}$$

in which the standard thermodynamic contributions, including the entropy per particle $s$, are complemented with a field $\mu_c$ that is conjugate to the microphase occupancy $n_c$ [46]. (This last quantity is generally proportional to the number of particles per period, but, for convenience, its specific definition here depends on the phase symmetry, e.g., area density $\varrho_\ell$ for lamellae of periodicity $\ell$, line density for cylinders and average cluster size $n_\mathcal{C}$ for cluster crystals.) Because in the thermodynamic $N \to \infty$ limit $\mu_c$ must vanish at equilibrium, optimal finite-size estimates have $\mu_c = 0$. Standard simulation schemes cannot, however, directly minimize this function because of the incommensurability between the mesoscale patterns and the simulation box in finite size system [44,57]. Hence, we first obtain the constrained free energy $f_c$ of a given microphase morphology at a given $(T, \rho)$ state point and fixed $n_c$ through a two-step thermodynamic integration (TI) scheme: (i) from an ideal gas to a liquid of hard spheres under a modulated field and (ii) from this last state to SWL particles without a field. The resulting constrained free energy is then optimized with respect to $n_c$ (Fig. 1) [46].

*Phase diagrams.*—The common tangent construction is used to obtain the coexistence boundaries between different phases and thus the overall phase diagram (Fig. 2). As expected, at high $T$ the system is disordered, while at low $T$ equilibrium microphases form. Four different ordered microphase morphologies are identified for $\rho \lesssim 0.45$: face-centered cubic (fcc) cluster crystal, cylindrical, double gyroid, and lamellar phases (see depictions in Fig. 2 and symmetry details in Ref. [46]). Although a Landau functional calculation for simple microphase formers suggests that a body-centered cubic (bcc) cluster crystal phase might also form [17,58], we found this structure to be only metastable in our system. The absence of the bcc symmetry suggests that the effective repulsion between clusters is harsher than $1/r^8$ [59–61], which a Hamaker-like calculation confirms [46]. This morphology thus appears to be more sensitive than others to the form of the interaction potential. The other microphase morphologies considered, i.e., $O^{70}$ [9], $P$-surface [62], ordered bicontinuous double diamond [63], and perforated lamellae [6], were all found to be unstable within the regime studied.

The highest temperature at which periodic microphases melt is the weakly first-order, order-disorder transition (ODT) [1,2]. This transition replaces the second-order gas-liquid critical point for systems beyond the Lifshitz point, i.e., for $\xi > \xi_L$ [16,46]. Melting of the periodic lamellae at $T_{\mathrm{ODT}}$ is monitored by the decay of the order parameter

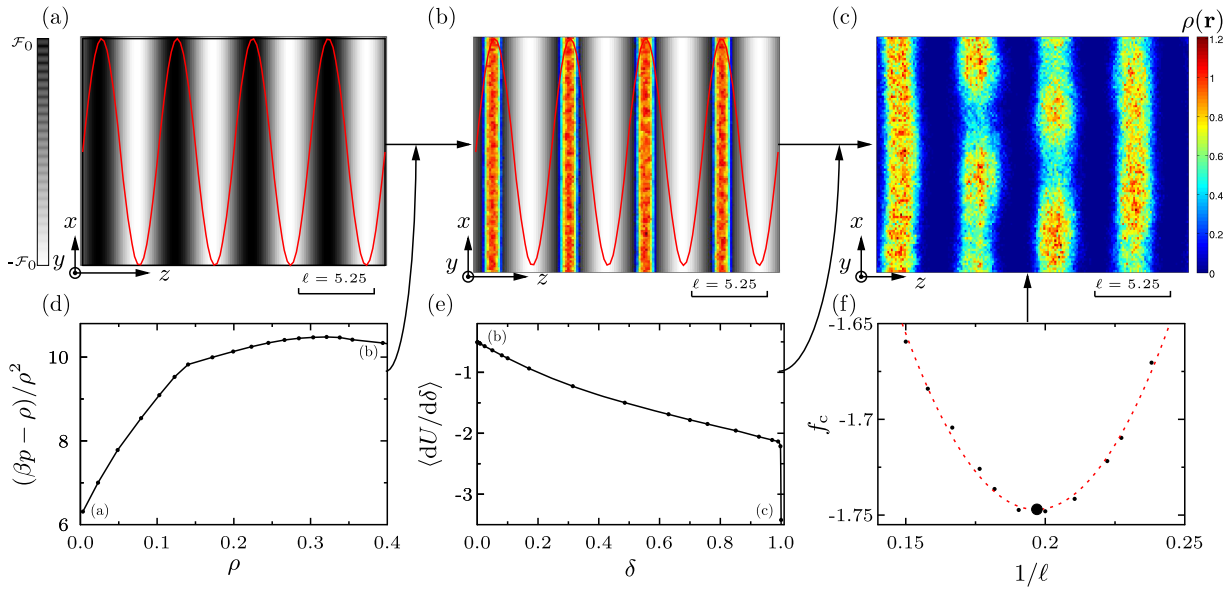


FIG. 1. Two-step TI for the lamellar phase at $T = 0.3$ and $\rho = 0.4$. Projections on the $xz$ plane of the coarse-grained number density $\rho(\mathbf{r})$ and external field profiles $\mathcal{F}(\mathbf{r})$ for (a) $\rho = 0$ with field $\mathcal{F}(\mathbf{r}) = \mathcal{F}_0 \cos(2\pi z/\ell)$, where $\mathcal{F}_0 = 2$ and $\ell = 5.25$, (b) $\rho = 0.4$ with a field, and (c) $\rho = 0.4$ without a field. Summing the TI results for the equation of state from (a) to (b) with those from the alchemical transformation in $\delta$ from (b) to (c) [46]—in (d) and (e), respectively—gives the free energy constrained to a given area density $\varrho_\ell = \rho\ell$ [46]. (f) From the minimum of a quadratic fit (dashed lines) to $f_c$ (points), we obtain the equilibrium thermodynamic $f$ at $\ell = \varrho_\ell/\rho = 5.05$ (large dot).

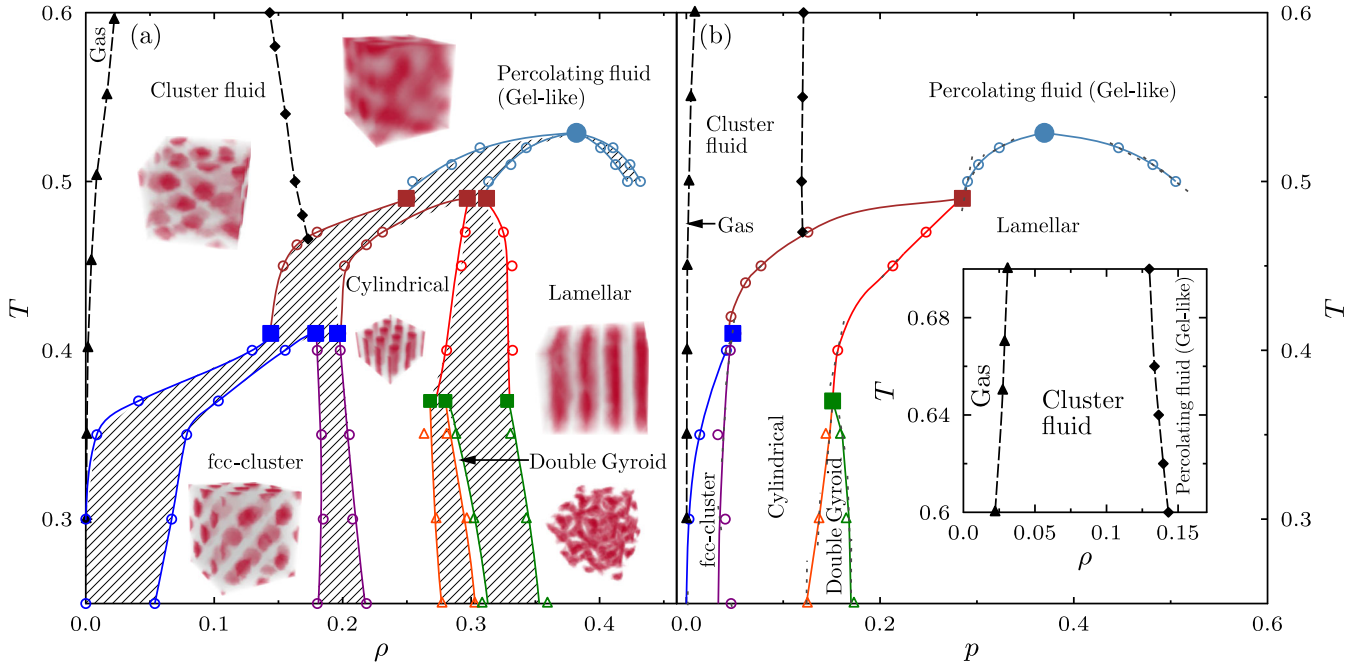


FIG. 2. Summary (a) $T-\rho$ and (b) $p-T$ phase diagrams indicating the first-order (empty symbols) and the order-disorder transition (solid circle) as well as the cmc (solid triangles) and percolation (solid diamonds) lines. Errors are comparable to the symbol sizes, striped areas correspond to coexistence regimes, and lines are guides for the eye. Clausius-Clapeyron results for the slope of the coexistence line (dashed lines) validate the numerical results in (b). Sample average density profiles for the different phases are given in (a). The inset provides percolation and cmc lines to higher $T$. Three triple points can be identified (solid squares): (i) fluid-fcc-cluster-cylindrical coexistence at $T=0.410(5)$ and $p=0.051(1)$, (ii) fluid-cylindrical-lamellar coexistence at $T=0.491(4)$ and $p=0.285(2)$, and (iii) cylindrical-double gyroid-lamellar coexistence at $T=0.37(1)$ and $p=0.15(1)$.

$$A(T)=\frac{1}{N}S(k^*;T), \tag{3}$$

where $k^*$ is the low-$k$ maximum of the structure factor $S(k;T)$. In our model, this transition occurs roughly halfway through the lamellar regime, at $\rho\approx 0.35$. Because $\varrho_\ell$, and thus $\ell$, is fairly independent of temperature in this regime [Fig. 3(a)], we use the $T=0.3$ value of $k^*\approx 2\pi/\ell$ to study the decay of $A(T)$. Simulation results indicate that, although away from the transition the order parameter behaves nearly critically, $A(T)$ vanishes discontinuously at $T_{\mathrm{ODT}}=0.535(5)$ [Fig. 3(b)]. Mechanistically, upon going through the transition, lamellae become increasingly flexible, giving rise to a percolated network, as observed in diblock copolymers [64].

At low temperatures, clusters form upon increasing density even before the onset of periodic microphase ordering, as reported in prior simulations and experiments [21,40]. The fluid equation of state allows us to locate the onset of clustering, which is akin to determining the critical micelle concentration (cmc) in a surfactant system [46]. Increasing $T$ along this line decreases the average cluster size $\bar{n}_{\mathrm{cmc}}$ [Fig. 3(c)], and the last hints of a cmc vanish around $T=0.72(1)$ [46]. Even within the fluid of clusters, the intracluster cohesion is relatively weak, resulting in the clusters' *internal* structure to also be fluidlike. This behavior contrasts with the crystallites observed in systems with shorter attraction ranges [27], but lowering the temperature may also lead to internally ordered clusters in this system. In spite of their internal fluidity, the clusters are not generally spherical, and their asphericity increases with $\rho$ [46]. For $T\gtrsim 0.45$, they even become wormlike and eventually percolate [46,65], which gels the system (see below) *before* the first-order transition into the periodic microphase regime is reached. This behavior is similar to that observed in Refs. [18,40] but contrasts with that of Ref. [27], where the percolating network was instead associated with incompletely ordered cylinder or lamellar phases. For $T\lesssim 0.45$, by contrast, cluster elongation is preempted by the microphase regime. Although this last transition is reminiscent of the crystallization of purely repulsive particles, the clusters in the fluid phase are larger [Fig. 3(d)] and display a much wider range of sizes and morphologies than those in the fcc-cluster crystal [44,46]. The fcc-cluster crystal assembly is thus expected to be more intricate than simple nucleation and growth.

We finally consider the percolated regime observed at temperatures above the periodic microphase regime. At $T\gg T_{\mathrm{ODT}}$ the system behaves like a regular fluid, but as $T$ approaches $T_{\mathrm{ODT}}$ the structural relaxation grows increasingly complex, even under the strongly nonlocal MC sampling we use here (Fig. 4): (i) Particles at the surface are a lot more mobile than those in the core [66,67], and (ii) edges of the network reorganize much faster than its nodes. Being in equilibrium, the system does not age, but MC sampling is nonetheless arduous [46], making the

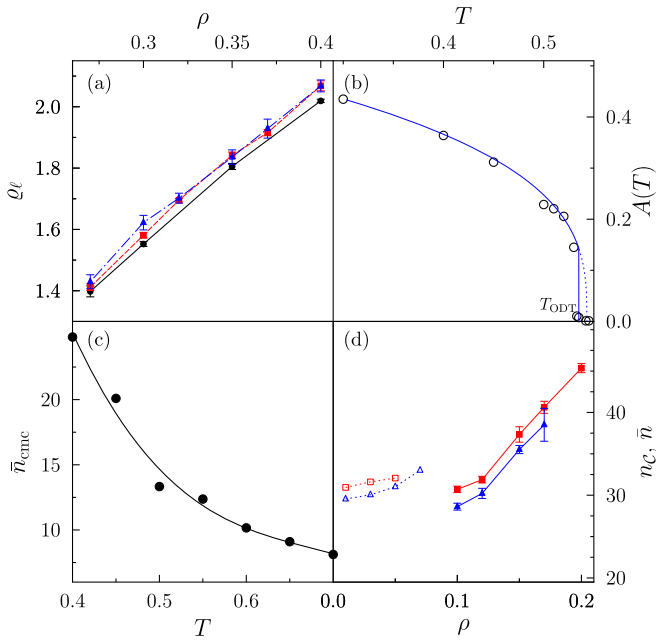


FIG. 3. (a) The equilibrium occupancy $\varrho_\ell$ of lamellae depends only weakly on temperature in this regime, where $T = 0.3$ (dots), $T = 0.35$ (squares), and $T = 0.4$ (triangles). (b) Decay of $A(T)$ at $\rho = 0.35$ (dashed line) fitted to an Ising critical form $A(T) \sim |1 - T/0.54|^{\beta_c}$ (solid line) with $\beta_c = 0.3264$ up to $T = 0.545$. We estimate $T_{\rm ODT} = 0.535(5)$. (c) The average cluster size at the cmc, $\bar{n}_{\rm cmc}$, decreases as $T$ increases (dots). The line is a guide for the eye. (d) Equilibrium fcc-cluster $n_{\mathcal{C}}$ (solid symbols) and average fluid cluster size $\bar{n}$ (empty symbols), at $T = 0.35$ (squares) and 0.40 (triangles). Because $\bar{n} > n_{\mathcal{C}}$ at the cluster fluid-fcc-cluster crystal transition, most clusters in the fluid must shrink for crystallization to proceed.

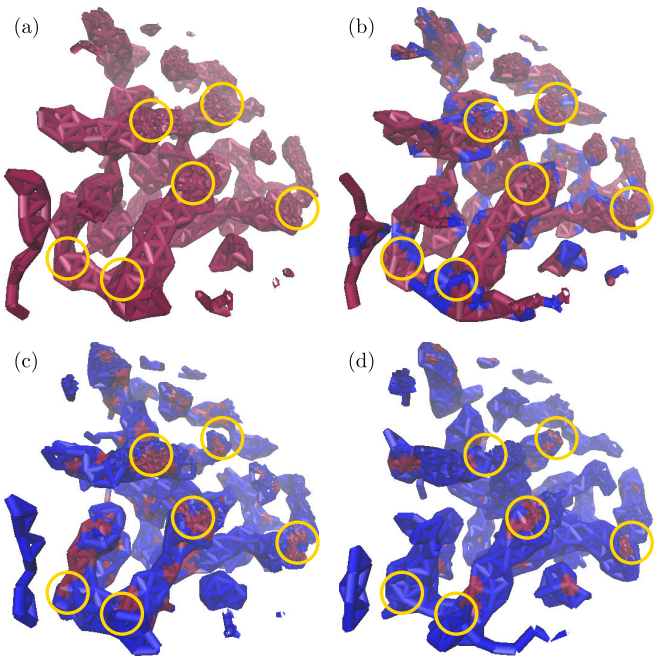


FIG. 4. Sample configuration slices after (a) 0, (b) 200, (c) 1600, and (d) 3200 MC sweeps of an initially equilibrated simulation with $N = 2000$ at $T = 0.45$ and $\rho = 0.2$. The distinction between particles that remain within $0.5\sigma$ of their initial conditions (red) and those that have moved beyond it (blue) illustrates the network dynamics. Surface particles decorrelate more rapidly than core particles, and network nodes (yellow circles) reorganize more slowly than network edges.

system gel-like. This multi-time-scale dynamics, in particular, the sluggish relaxation of network nodes, may contribute to the difficulty of assembling microphases in colloids [25,26]. Note that other mechanisms slowing down the dynamics could also emerge below $T_{\rm ODT}$, including competing microphase morphologies [30–32] and spinodal-like arrest [27–29], but a systematic study of these nonequilibrium effects is left for future consideration.

*Conclusion.*—We have developed a TI-based simulation method for solving the phase diagram of arbitrary continuous-space microphase-forming models. Our solution of the prototypical SWL model presents the periodic microphase sequence—cluster crystal, cylindrical, double gyroid, and lamellar phases—of systems described by a comparable Landau functional [17]. Our search for ordered phases, however, was not exhaustive; hence, other stable morphologies are possible. More importantly, we have clarified the thermodynamic interplay between fluids of spherical and wormlike clusters, the equilibrium percolating fluid (gel-like), and periodic microphases. This distinction is essential for separating equilibrium from nonequilibrium effects in the dynamical arrest of microphase formers [17,25,27,29]. It is also essential for guiding experiments with SALR-like colloidal interactions, whose precise form can vary with system density [68]. Indeed, colloidal experiments have thus far identified only equilibrium cluster fluids and gels [18–21,40]. Whether the challenge of assembling ordered microphases in colloids could be surmounted by tuning the properties of these disordered regimes or by identifying alternate assembly pathways remains, however, an open question.

We acknowledge many stimulating discussions about this project over the years, in particular, with A. Ciach, E. Del Gado, D. Frenkel, P. Royall, and S. Yaida. We acknowledge support from the National Science Foundation Grant No. NSF DMR-1055586.

[1] M. Seul and D. Andelman, Science **267**, 476 (1995).
[2] F. S. Bates and G. H. Fredrickson, Annu. Rev. Phys. Chem. **41**, 525 (1990).
[3] F. S. Bates and G. H. Fredrickson, Phys. Today **52**, No. 02, 32 (1999).
[4] H.-C. Kim, S.-M. Park, and W. D. Hinsberg, Chem. Rev. **110**, 146 (2010).
[5] L. Leibler, Macromolecules **13**, 1602 (1980).
[6] M. W. Matsen and F. S. Bates, Macromolecules **29**, 1091 (1996).

[7] R. J. Spontak, S. D. Smith, and A. Ashraf, Macromolecules **26**, 956 (1993).
[8] T. Epps, E. Cochran, and T. Bailey, Macromolecules **37**, 8325 (2004).
[9] C. A. Tyler and D. C. Morse, Phys. Rev. Lett. **94**, 208302 (2005).
[10] E. J. Crossland *et al.*, Nano Lett. **9**, 2807 (2009).
[11] M. R. J. Scherer, in *Sythesis and Applications*, Springer Theses (Springer, Heidelberg, 2013), pp. 7–20.
[12] K. Kataoka, A. Harada, and Y. Nagasaki, Adv. Drug Delivery Rev. **47**, 113 (2001).
[13] A. Rösler, G. W. Vandermeulen, and H.-A. Klok, Adv. Drug Delivery Rev. **64**, 270 (2012).
[14] M. Q. Li and C. K. Ober, Mater. Today **9**, 30 (2006).
[15] S. Krishnamoorthy, C. Hinderling, and H. Heinzelmann, Mater. Today **9**, 40 (2006).
[16] S. A. Brazovskii, JETP Lett. **41**, 85 (1975).
[17] A. Ciach, J. Pekalski, and W. T. Góźdź, Soft Matter **9**, 6301 (2013).
[18] A. I. Campbell, V. J. Anderson, J. S. van Duijneveldt, and P. Bartlett, Phys. Rev. Lett. **94**, 208301 (2005).
[19] C. L. Klix, C. P. Royall, and H. Tanaka, Phys. Rev. Lett. **104**, 165702 (2010).
[20] T. H. Zhang, J. Klok, R. Hans Tromp, J. Groenewold, and W. K. Kegel, Soft Matter **8**, 667 (2012).
[21] A. Stradner, H. Sedgwick, F. Cardinaux, W. C. Poon, S. U. Egelhaaf, and P. Schurtenberger, Nature (London) **432**, 492 (2004).
[22] E. Jordan, F. Roosen-Runge, S. Leibfarth, F. Zhang, M. Sztucki, A. Hildebrandt, O. Kohlbacher, and F. Schreiber, J. Chem. Phys. **118**, 11365 (2014).
[23] J. Schmalian and P. G. Wolynes, Phys. Rev. Lett. **85**, 836 (2000).
[24] P. L. Geissler and D. R. Reichman, Phys. Rev. E **69**, 021501 (2004).
[25] J. C. F. Toledano, F. Sciortino, and E. Zaccarelli, Soft Matter **5**, 2390 (2009).
[26] H. Liu, S. Garde, and S. Kumar, J. Chem. Phys. **123**, 174505 (2005).
[27] A. de Candia, E. Del Gado, A. Fierro, N. Sator, M. Tarzia, and A. Coniglio, Phys. Rev. E **74**, 010403 (2006).
[28] M. Tarzia and A. Coniglio, Phys. Rev. E **75**, 011410 (2007).
[29] P. Charbonneau and D. R. Reichman, Phys. Rev. E **75**, 050401(R) (2007).
[30] C.-Z. Zhang and Z.-G. Wang, Phys. Rev. E **73**, 031804 (2006).
[31] A. de Candia, A. Fierro, and A. Coniglio, J. Stat. Phys. **145**, 652 (2011).
[32] E. Del Gado and W. Kob, Soft Matter **6**, 1547 (2010).
[33] M. W. Matsen and M. Schick, Phys. Rev. Lett. **72**, 2660 (1994).
[34] A. Imperio and L. Reatto, J. Phys. Condens. Matter **16**, S3769 (2004).
[35] A. J. Archer and N. B. Wilding, Phys. Rev. E **76**, 031501 (2007).
[36] R. P. Sear and W. M. Gelbart, J. Chem. Phys. **110**, 4582 (1999).
[37] B. Ruzicka, L. Zulian, and G. Ruocco, Phys. Rev. Lett. **93**, 258301 (2004).
[38] M. Tarzia and A. Coniglio, Phys. Rev. Lett. **96**, 075702 (2006).
[39] L. Berthier and G. Biroli, Rev. Mod. Phys. **83**, 587 (2011).
[40] F. Sciortino, S. Mossa, E. Zaccarelli, and P. Tartaglia, Phys. Rev. Lett. **93**, 055701 (2004).
[41] R. B. Jadrich, J. A. Bollinger, K. P. Johnston, and T. M. Truskett, Phys. Rev. E **91**, 042312 (2015).
[42] T. H. Zhang, B. W. M. Kuipers, W.-D. Tian, J. Groenewold, and W. K. Kegel, Soft Matter **11**, 297 (2015).
[43] K. Binder and M. Müller, Curr. Opin. Colloid Interface Sci. **5**, 314 (2000).
[44] B. M. Mladek, P. Charbonneau, and D. Frenkel, Phys. Rev. Lett. **99**, 235702 (2007).
[45] M. Müller and K. C. Daoulas, J. Chem. Phys. **128**, 024903 (2008).
[46] See Supplemental Material at http://link.aps.org/supplemental/10.1103/PhysRevLett.116.098301 for an extended consideration of the periodic microphase and cluster regimes as well as the simulation details, which includes Refs. [47, 48].
[47] W. M. Gelbart, A. Ben-Shaul, and D. Roux, *Micelles, Membranes, Microemulsions, and Monolayers* (Springer Science, New York, 2012).
[48] J. N. Israelachvili, *Intermolecular and Surface Forces*, revised third edition (Academic, New York, 2011).
[49] D. Pini, G. Jialin, A. Parola, and L. Reatto, Chem. Phys. Lett. **327**, 209 (2000).
[50] H. W. Diehl and M. Shpot, Phys. Rev. B **62**, 12338 (2000).
[51] A. J. Schultz and D. A. Kofke, Phys. Rev. E **84**, 046712 (2011).
[52] B. Chen and J. I. Siepmann, J. Chem. Phys. **104**, 8725 (2000).
[53] D. Frenkel and B. Smit, *Understanding Molecular Simulation* (Academic press, London, 2002).
[54] S. Whitelam and P. L. Geissler, J. Chem. Phys. **127**, 154101 (2007).
[55] K. Zhang and P. Charbonneau, J. Chem. Phys. **136**, 214106 (2012).
[56] W. C. Swope and H. C. Andersen, Phys. Rev. A **46**, 4539 (1992).
[57] N. Wilding, J. Stat. Phys. **144**, 652 (2011).
[58] A. Ciach, Phys. Rev. E **78**, 061505 (2008).
[59] R. Agrawal and D. A. Kofke, Phys. Rev. Lett. **74**, 122 (1995).
[60] K. Zhang and P. Charbonneau, Phys. Rev. B **83**, 214303 (2011).
[61] K. Zhang, P. Charbonneau, and B. M. Mladek, Phys. Rev. Lett. **105**, 245701 (2010).
[62] W. T. Góźdź and R. Hołyst, Phys. Rev. E **54**, 5012 (1996).
[63] K. I. Winey, E. L. Thomas, and L. J. Fetters, Macromolecules **25**, 422 (1992).
[64] O. Portmann, A. Vaterlaus, and D. Pescia, Phys. Rev. Lett. **96**, 047212 (2006).
[65] D. Stauffer and A. Aharony, *Introduction to Percolation Theory* (CRC Press, Boca Raton, 1994).
[66] S. Wu, H. W, Jr., J. Schmalian, and P. G. Wolynes, Chem. Phys. Lett. **359**, 1 (2002).
[67] J. D. Stevenson and P. G. Wolynes, J. Chem. Phys. **129**, 234514 (2008).
[68] C. L. Klix, K.-i. Murata, H. Tanaka, S. R. Williams, A. Malins, and C. P. Royall, Sci. Rep. **3**, 2072 (2013).